Downloaded from orbit.dtu.dk on: Aug 09, 2024

DTU Library

Core density profile control by energetic ion anisotropy in LHD

Nishiura, M.; Shimizu, A. ; Ido, T.; Satake, S.; Yoshinuma, M.; Yanai, R. ; Nunami, M. ; Yamaguchi, H.; Nuga, H. ; Seki, R.

Total number of authors:
12

Published in:
Physics of Plasmas

Link to article, DOI:
10.1063/5.0201440

Publication date:
2024

Document Version
Publisher's PDF, also known as Version of record

Link back to DTU Orbit

Citation (APA):
Nishiura, M., Shimizu, A., Ido, T., Satake, S., Yoshinuma, M., Yanai, R., Nunami, M., Yamaguchi, H., Nuga, H., Seki, R., Fujita, K., & Salewski, M. (2024). Core density profile control by energetic ion anisotropy in LHD. *Physics of Plasmas*, *31*, Article 062505. https://doi.org/10.1063/5.0201440

General rights
Copyright and moral rights for the publications made accessible in the public portal are retained by the authors and/or other copyright owners and it is a condition of accessing publications that users recognise and abide by the legal requirements associated with these rights.

- Users may download and print one copy of any publication from the public portal for the purpose of private study or research.
- You may not further distribute the material or use it for any profit-making activity or commercial gain
- You may freely distribute the URL identifying the publication in the public portal

If you believe that this document breaches copyright please contact us providing details, and we will remove access to the work immediately and investigate your claim.

Physics of Plasmas ARTICLE pubs.aip.org/aip/pop

Core density profile control by energetic ion anisotropy in LHD

Cite as: Phys. Plasmas **31**, 062505 (2024); doi: 10.1063/5.0201440
Submitted: 30 January 2024 · Accepted: 19 May 2024 ·
Published Online: 5 June 2024

View Online Export Citation CrossMark

M. Nishiura,[1,2,a),b)] A. Shimizu,[1] T. Ido,[3] S. Satake,[1] M. Yoshinuma,[1] R. Yanai,[1] M. Nunami,[1] H. Yamaguchi,[1] H. Nuga,[1] R. Seki,[1] K. Fujita,[4] and M. Salewski[5]

AFFILIATIONS

[1]National Institute for Fusion Science, 322-6 Oroshi, Toki, 509-5292 Gifu, Japan
[2]Graduate School of Frontier Sciences, The University of Tokyo, Kashiwa 277-8561, Japan
[3]Department of Advanced Energy Engineering, Kyushu University, Kasuga, Fukuoka 816-8580, Japan
[4]Department of Physics, Nagoya University, Chikusa, Nagoya 464-8601, Japan
[5]Department of Physics, Technical University of Denmark, Lyngby, Denmark

Note: This paper is part of the Special Collection: Papers from the 65th Annual Meeting of the APS Division of Plasma Physics.
Note: Paper YI1 1, Bull. Am. Phys. Soc. **68** (2023).
[a)]Invited speaker.
[b)]**Author to whom correspondence should be addressed:** nishiura@nifs.ac.jp

ABSTRACT

Electron and impurity ion density profiles have been controlled by using tangential and perpendicular neutral beams for plasma heating in a stellarator/heliotron for the first time. Reduced anisotropy of stored energy for energetic ion $En_{\perp}/En_{||}$ has resulted in an inward electron and impurity transport, forming a core electron density peaking. Increased anisotropy leads to a flat or hollowed electron density profile with an impurity exhaust in a core region [Yoshinuma *et al.*, Nucl. Fusion **49**, 062002 (2009)]. A high confinement state of particles in LHD has yet to be achieved, except for a temporal state of an electron density peaking created by a pellet injection. As a pioneering and crucial research result, the operation of energetic ion anisotropy by neutral beams has newly demonstrated that the direction of the radial transport of bulk and impurity ions can be controlled. At the same time, the overall plasma performance rises in neutron flux and stored energy. On the other hand, the increase in the anisotropy flattens the density profile. This new finding holds promise for a control knob of nuclear fusion reactors to enhance fusion power output.

© 2024 Author(s). All article content, except where otherwise noted, is licensed under a Creative Commons Attribution (CC BY) license (https://creativecommons.org/licenses/by/4.0/). https://doi.org/10.1063/5.0201440

05 June 2024 09:58:47

I. INTRODUCTION

Experimental and theoretical studies on thermal and particle transport in fusion plasmas have been intensively carried out because of their impact on the performance of fusion reactors.[1,2] The transport process is believed to be due to the balance between turbulent transport and collisional transport based on neoclassical theory. Mazzi *et al.* reported the influence of transport for thermal ions and electrons on the energetic ions in JET Tokamak plasmas. They found that generating large-scale zonal flow suppresses excited turbulence.[3] Han *et al.* also report that the abundant population of fast ions suppresses the core plasma turbulence in a reactor-relevant condition in KSTAR.[4] Most experimental and theoretical studies focused on a bulk plasma transport. Self-burning plasma contains abundant alpha particles with mega-electron volt energies in the plasma. In such a situation, the excitation of microinstabilities or turbulence and the particle and energy transports caused by its effect should be clearly understood.

In the LHD, impurity exhausting has been observed, and transport analysis of the driving force and radial direction indicates that bulk ions have small positive convection. In contrast, impurity carbon ions have a relatively large convection velocity.[5,6] The sign of the convection velocity was positive, contrary to the neoclassical theory prediction. Experimental results were also reported on the relation between the torque input by neutral beam (NB) particles from the NB injector and the peaking and exhaust of impurity ions. As the gradient of bulk ion temperature increases, the impurity ions maintain a hollow profile for zero torque input. Progress has been made in global calculations of neoclassical transport theory in LHD plasmas.[7] The simulation includes the non-uniformity of the electrostatic potential on the

© Author(s) 2024

magnetic flux surface of the LHD as Φ_1 enhances the outward flux of impurities and allows a rigorous discussion of particle transport, which has, to our knowledge, not been reported previously. In addition to transport studies of bulk and impurity ions using carbon pellets, it is reported that the injection of submillimetric boron power grains into the plasmas in the LHD improves radial heat conductivity.[8] Global gyrokinetic simulations are used to qualitatively explain the experimental thermal conductivity in such situations.[9]

The electron density profiles were either flat or hollow in these transport experiments, where impurity density exhaust was observed in the LHD. A pellet injection forms peaked density profiles, but an electron density profile returns to a flat or hollow shape in a steady state eventually. The reason for the sustainment of a centrally peaked density profile, as in tokamak plasmas, could be due to differences in particle recycling in the periphery and a unique rotational transform for the LHD. The problem for the density profile still needs to be satisfactorily explained. In this paper, we point out that the anisotropy of energetic ions in the velocity space is essential for the density profile and the particle transport. As far as we understand, there has yet to be a report from this point of view.

II. DENSITY PEAKING AND FLATTENING BY ANISOTROPIC ENERGETIC IONS

The LHD utilizes superconducting magnets to form a heliotron-type magnetic configuration,[10] which is used for steady-state plasma and various plasma research. It is equipped with unique tangential neutral beam (NB) injectors with an injection energy of ∼190 keV and perpendicular NB injectors with an injection energy of ∼80 keV for plasma production and heating. The energetic ion population with parallel and perpendicular velocities originated from NBs is due to the geometries of the beamlines of NBs with respect to the magnetic field. The energetic ions deposited exist with the mixed parallel and perpendicular velocity components in plasmas. The geometries of NBs, a pellet injector, and a heavy ion beam probe (HIBP) in LHD are shown in Fig. 1. A method for capturing the characteristics of the

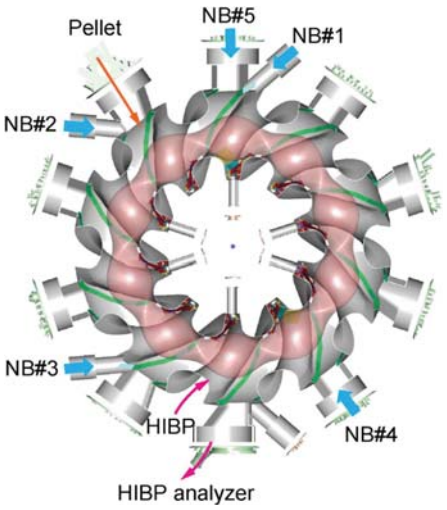

FIG. 1. LHD vacuum vessel and plasma viewed from the top, showing the locations of NBs, pellet, and HIBP.

two-dimensional velocity distribution function from the one-dimensional one of energetic ions has been proposed.[11,12] Because energetic ions are anisotropic due to plasma heating, measurement signals related to the 1D velocity distribution function of CTS and FIDA must be transformed by this tomographic method to obtain the 2D distribution function at a certain location. The feature of energetic ions distributed in the velocity space is better understood from simulations as well as by measurements using a collective Thomson scattering diagnostic.[13–15] The tangential and perpendicular NBs can be utilized to investigate particle transport, which determines a stable density profile from a transient profile. Energetic ions may also provoke or suppress turbulence and the effect of turbulence on the global transport of thermalized ions and electrons.

The configuration of the LHD is set to the magnetic axis $R_{ax} = 3.6$ m and the toroidal magnetic field $B_t = 2.75$ T. Figure 2 shows the electron density profiles for the peaking cases in shots #182 736 and #182 744 and the flattening case in #182 745 at $t = 5.3003$ s, while the shapes of the ion and electron temperature profiles are almost the same. Neutral beam heating sustains plasma discharges with the tangential and the perpendicular NBs, where the tangential NB power $P_{||}$ comes from Ctr-NB#1, Co-NB#2, and Ctr-NB#3, and the perpendicular NB power comes from $P_\perp$ for NB#4 and NB#5. The beam energies for the perpendicular and the tangential NBs are fixed at 80 and 190 keV, respectively, while the beam currents of ion sources are controlled to change $P_\perp$ and $P_{||}$ for the experiments. When a carbon pellet is injected into the plasma at $t = 3.8$ s, the electron and impurity density reach a steady state at $t = 4.5$ s. The main impurity is carbon ions produced from a pellet in this experiment. The pellets are used to study impurity transport and to aid in the observation of carbon emission for a charge exchange recombination spectroscopy (CXRS) in the core region. The carbon pellet is a cylindrical shape with 1 mm in diameter and 1 mm in length and produces 9.0×10^{19} atoms. The pellet is injected at about 200 m/s horizontally from the 10-O port of the equatorial plane of the LHD toward the center of the major radius.[16] The electron and ion temperatures at the center are $T_{e0} = 2.5$ and $T_{i0} = 5$ keV, respectively. In shots #182 736 and #182 744, impurity carbon accumulates in the center of the plasma, whereas in shot #182 745, impurity carbon is exhausted in the center of the plasma, and the electron density is flattened.

The novel peaking case only increases the perpendicular NB power, whereas the discharge conditions in the flattening case (#182 745) are similar to those reported in previous transport studies.[5,6] The input NB powers are summarized in Table I. As the $P_\perp/P_{||}$ ratio increases to more than 1.7, the peaked density profiles for electron and impurity carbon ions are created. In contrast, the flattened and hollow profiles are formed at the reduced $P_\perp/P_{||}$ ratio of 1.2.

To understand how the anisotropy of energetic ions in velocity space affects the density profile and particle and heat transport, the use of the perpendicular and the parallel stored energies for energetic ions $En_\perp$ and $En_{||}$ is more suitable than that of $P_\perp$ and $P_{||}$ ratio from the NB powers because $P_\perp$ and $P_{||}$ produce mainly energetic ions with perpendicular and parallel pitch angles, respectively; however, they contain various pitch angles after deposition to an extent. We use the FIT3d code[17] with the slowing down process for energetic ions. The effect of the energetic ion anisotropy on the density profile is examined by changing the ratio of $En_\perp/En_{||}$. The electron and carbon densities n_e and n_c, and their gradients dn_e/dr and dn_c/dr are plotted as a

05 June 2024 09:58:47

© Author(s) 2024

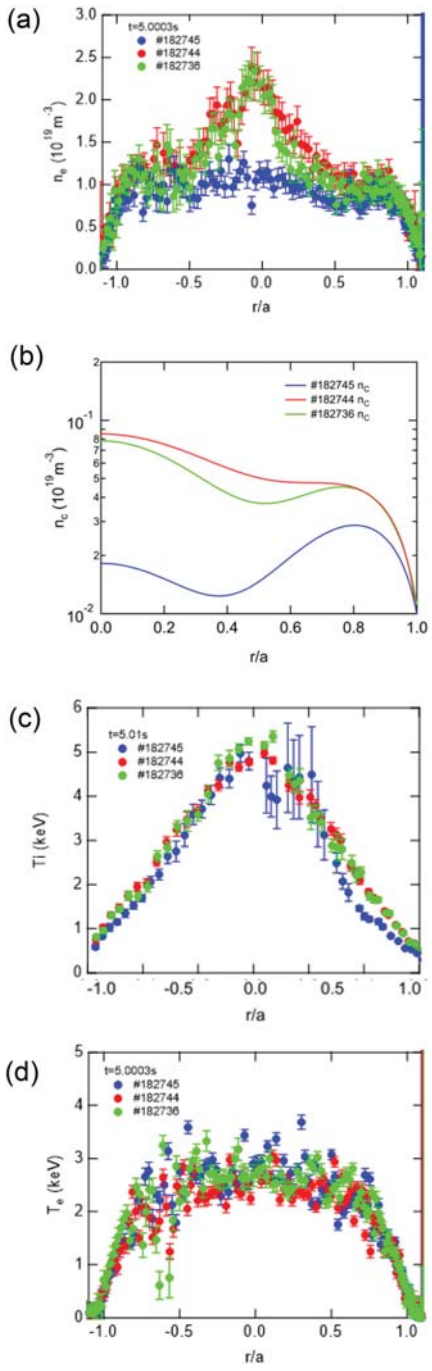

FIG. 2. The energetic ion anisotropy changes density profiles with peaking in #182 736 (Ctr-NB#1, Co-NB#2, Ctr-NB#3, perp. NB#5 full, $P_\perp/P_{||} = 1.7$) and #182 744 (Ctr-NB#1, Co-NB#2, perp. NB#5 full, $P_\perp/P_{||} = 2.6$, the injection powers of Ctr-NB#1 and Co-NB#2 are balanced to cancel a plasma current), and with flattening in #182 745 (Ctr-NB#1, Co-NB#2, Ctr-NB#3, perp. NB#5 half, $P_\perp/P_{||} = 1.2$). The profiles for (a) the electron density, (b) the impurity carbon density, (c) the ion temperature, and (d) the electron temperature. The peak and hollow profiles of impurity carbon are varied by the ratio of $P_\perp/P_{||}$.

TABLE I. Input of NB powers and its ratios for anisotropy index.

	$P_\perp$ (MW)	$P_{||}$ (MW)	$P_\perp/P_{||}$	$En_\perp/En_{||}$	
#182 736	14.0	8.1	1.7	0.47	Peaked
#182 744	14.0	5.4	2.6	0.77	Peaked
#182 745	9.9	8.2	1.2	0.35	Flattened

function of $En_\perp/En_{||}$ in Fig. 3. Here, dn_e/dr is obtained by an electron density profile from Thomson scattering measurement at r/a = 0–0.2. We chose the gradient inside r/a = 0.5, where the difference in profiles appears and where the particle transport changes. dn_c/dr is by a carbon density profile calculated from CXRS measurement, as shown in Fig. 2(b). $En_\perp/En_{||}$ was increased from 0.3 to 0.8 by varying $En_\perp$ at the same density and temperature conditions. The results show that for $En_\perp/En_{||} < 0.35$, n_e has a flat profile and n_c has a hollow profile, the so-called "impurity hole" state; for $En_\perp/En_{||} \sim 0.4$, dn_e/dr and dn_c/dr change steeply to peaked profiles. The peaked profiles for electrons and impurity carbon are sustained even at the more isotropic energetic ion pressure $En_\perp/En_{||} = 0.75$. From the transport analysis in Refs. 5 and 6, the inward and outward fluxes for bulk and impurity ions are driven by convective flows. The low $En_\perp/En_{||}$ regime (less than 0.4), where the Refs. 5 and 6 examined the particle transport, results in a flattening profile for electrons and a hollow profile for impurity carbon ions. In contrast, the novel $En_\perp/En_{||}$ regime (more than 0.47 or higher) can access an inward flux state such as peaked density profiles. Controlling the particle directions leads to a novel concept of particle control in the burning plasmas of nuclear fusion reactors.

For the comparison between the density peaking case (#182 736) and flattening case (#182 745), the overall confinement performance of the neutron flux and the stored energy increase by approximately 20% for the density peaking case.

Varying the power of the NB in the tangential direction, a flattening of the density was observed at $P_\perp/P_{||} = 1.02$ for #171 000 and peaking of the density at $P_\perp/P_{||} = 2.07$ for #170 997. The radial flux

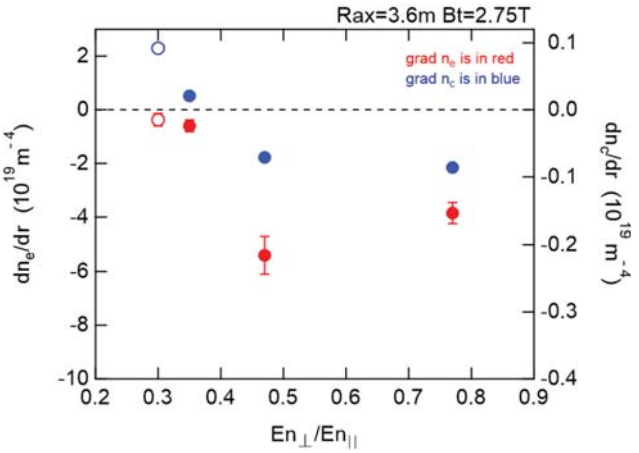

FIG. 3. Dependence of density gradients for bulk (red circles) and impurity carbon ions (blue circles) on the $En_\perp/En_{||}$. All NBs inject D beams, and the LHD uses D_2 gas puff. Tangential NBs inject H beams (open circles) and D_2 gas puff.

05 June 2024 09:58:47

© Author(s) 2024

direction is influenced by $P_\perp/P_{||}$, resulting in an inflow at $P_\perp/P_{||} = 1.76–2.07$ and an outflow dominated at $P_\perp/P_{||} = 1.02–1.2$. The particle transport is significantly affected by changes in density and temperature due to a pellet injection. We have confirmed that the density peaking occurs at $P_\perp/P_{||} = 1.31$, even in #182 723, where no pellets are injected.

III. RADIAL ELECTRIC FIELD IN DENSITY PEAKING AND FLATTENING

In the case of density peaking, the electrostatic potential ϕ in the plasma core region is measured by the HIBP for shot #182 737. The measurement position is fixed at $r/a = 0.2$ to track the time evolution of ϕ after a pellet injection. ϕ is positive from $t = 3.0$ to 3.5 s due to electron cyclotron heating. At $t = 3.7$ s, the plasma is sustained only by the perpendicular NB#4 and NB#5, and ϕ is negative. When the carbon pellet is injected at $t = 3.8$ s, the electron density increases rapidly to more than $2 \times 10^{19}\,m^{-3}$. The tangential NBs #1–#3 are injected at $t = 4.0$ s, and ϕ is negative. ϕ becomes slightly negative or nearly zero and a steady state at $t = 5.0$ s.

The HIBP measures the spatial profiles of ϕ in Fig. 4 to evaluate the radial electric field Er. In impurity hole phenomena, negative Er is formed in the core region and positive Er in the peripheral region.[18] The electrostatic potential profiles ϕ(r/a) of #182 745 (flattened profile) and #182 744 (peaked profile) were measured at t = 5.1 s. Shot #182 745 has Er = −5 kV/m, consistent with previous measurements. ϕ(r/a) is relatively higher for #182 745 than for #182 744 in the range $0 < r/a < 0.3$. The Er obtained from the measured potential profile is Er = −5 kV/m at $r/a < 0.3$ for #182 745. Er = −5 kV/m at $r/a < 0.3$ and Er = 0 kV/m at r/a = 0.33–0.5 for #182 744.

We have examined Er profiles for other shots with peaked and flat-density profiles. However, we have yet to obtain sufficient results to explain the difference in density profile shape depending on the transport state. For $r/a > 0.5$, density peaking and flattening due to Er may have a substantial effect. However, since the Er that HIBP can evaluate is limited to the region of $r/a < 0.5$, we investigated whether the difference in experimental density profile can be explained by thermal particle transport analysis based on neoclassical and turbulence theories, including the region that HIBP cannot measure. The current FORTEC-3D code can calculate neoclassical electric field using measured plasma parameters and plasma equilibrium for bulk electrons and ions with an isotropic Maxwell distribution. However, the anisotropic distribution function of energetic ions cannot be treated in this code as well as plasma equilibrium. Therefore, to evaluate the effect of the ambipolar Er on energetic ions, we use the GNET code[19] with neoclassical module DGN/LHD.[20] The GNET code solves the drift kinetic equation for fast ions produced by NBs in 5D phase space, considering the impurity collisions and the complex guiding-center motion. The module DGN/LHD can evaluate the neoclassical Er produced by thermal bulk ions and anisotropic energetic ions calculated by the GNET code. Figure 5 shows the simulation results for shots #182 744 (peaked density profile) and #182 745 (flattened density profile). In both cases of peaked and flat density profiles, the calculation including only the effect of bulk ions shows little change in the profile of Er, with Er = −5 kV/m at around r/a = 0.3. When the effect of energetic ions is included, Er = −10 kV/m at r/a = 0.3–0.5 for the peaked distribution, while for the flat distribution, Er remains negative and almost unchanged. The difference in Er with and w/o energetic ions for both shots is −5 kV/m, comparable to the measured Er by the HIBP. At $r/a > 0.6$, the simulation results indicate no apparent effect

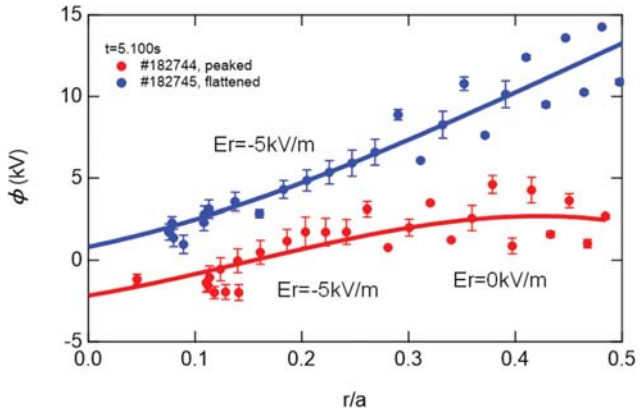

FIG. 4. Electric potential profiles measured by the HIBP at t = 5.100 s for #182 744 (peaked) and #182 745 (flattened).

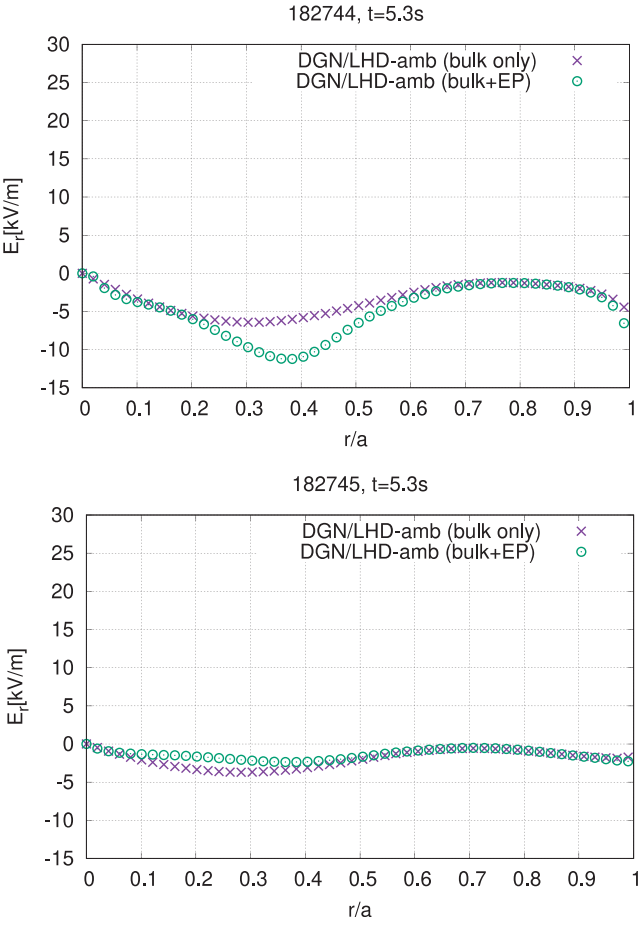

FIG. 5. Energetic ion effect on neoclassical Er for #182 744 (peaked) and #182 745 (flattened) at t = 5.3 s.

05 June 2024 09:58:47

© Author(s) 2024

of energetic ion anisotropy on Er. In addition, Er would be too small to change the bulk ion transport.

IV. TURBULENT TRANSPORT ANALYSIS

Since this experiment is performed in the $1/\nu$ region of low collision frequencies, the balance between turbulence and the neoclassical transports is expected to determine the direction of the driving force. Therefore, the gyrokinetic Vlasov simulation code GKV[21] analyzes the turbulent state of plasmas as a local simulation to understand the turbulent behavior. Figure 6 shows the linear growth rate γ and the real frequency ω based on micro instability for each of the three cases shown previously. Here, we evaluated γ at $r/a = 0.5$, where the foot point of the peaked density profiles is located. From the results, it can be seen that γ becomes unstable in all cases. The highest γ is for #182 745, where the density profile flattens. The calculated ω is about the same for the peaked and flattened profiles #182 745 and #182 736, respectively, and lower for the peaked profile #182 744. Since ω may be affected by the impurity profile and density gradient, it seems insufficient to conclude from the local $r/a = 0.5$ alone. As for the heat and particle transport that determines the density distribution, destabilized turbulence is thought to determine the radial transport. Therefore, detailed particle transport analysis should be performed using the neoclassical transport code FORTEC-3D[7] and the nonlinear turbulent transport code GKV. In addition to the turbulent effect in these discharges, energetic ions excite MHD activity, which magnetic probes observe. However, the spectrogram analysis showed no apparent difference in frequency and intensity. From the FIT3d results, it is found that the fueling effect supplied from NBs is one order of magnitude lower than the electron density and cannot explain the density peaking.

V. SUMMARY

In LHD plasma experiments, we have investigated the anisotropy of energetic ions on the velocity space. The anisotropic state can change the confinement states of electrons and impurities in the core plasmas. It was then revealed that we entered a novel particle confinement regime at LHD. Reducing the anisotropy $En_\perp/En_{||}$ (approaching 1) of the stored energy of energetic ions promotes inward particle transport. The present experiments show for the first time that controlling the anisotropy of energetic ions in velocity space in the core plasma of LHD maintains a peaked electron density distribution. This result is a significant advance since the high confinement state of particles in conventional LHD plasmas is only achieved by a temporary density peaking using pellet injection. The measured Er was negative at -5 kV/m for $r/a < 0.5$ for both peaked and flattened density profiles and was comparable to Er produced by energetic ions with the GNET code, indicating that the code does not significantly change the predicted transport. The linear growth rate by gyrokinetic theory is positive, suggesting that turbulence-induced instabilities are being excited.

Further nonlinear GKV analysis is needed to gain insight into particle transport due to the anisotropy of energetic ions. This novel and essential discovery is a common physics in toroidal plasmas. Because of the abundance of energetic ions in fusion plasmas, it has the potential to alter the confinement of the main plasma and impurities significantly. It is also expected that the anisotropy plays the role of a new particle transport control knob.

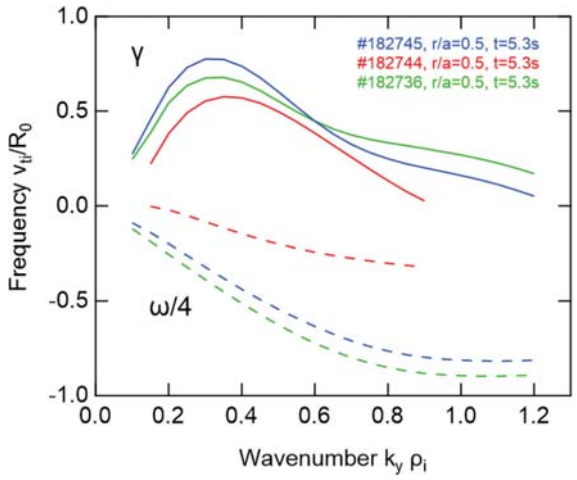

FIG. 6. Linear growth rates γ (curves) and real frequencies $\omega/4$ (dotted curves) for #182 736 (peaked), #182 744 (peaked), and #182 745 (flattened).

ACKNOWLEDGMENTS

This work was supported by the JSPS KAKENHI under Grant Nos. 19KK0073 and 23H01160. We would like to thank the LHD experiment group for their generous experimental support and fruitful discussions.

AUTHOR DECLARATIONS

Conflict of Interest

The authors have no conflicts to disclose.

Author Contributions

M. Nishiura: Conceptualization (lead); Data curation (lead); Formal analysis (lead); Funding acquisition (lead); Investigation (lead); Methodology (lead); Project administration (lead); Writing – original draft (lead); Writing – review & editing (lead). **A. Shimizu:** Methodology (equal). **T. Ido:** Formal analysis (equal). **S. Satake:** Data curation (equal); Methodology (equal). **M. Yoshinuma:** Data curation (equal). **R. Yanai:** Methodology (equal). **M. Nunami:** Formal analysis (equal). **H. Yamaguchi:** Formal analysis (equal). **H. Nuga:** Formal analysis (equal). **R. Seki:** Formal analysis (equal). **K. Fujita:** Formal analysis (equal). **M. Salewski:** Writing – original draft (supporting); Writing – review & editing (supporting).

DATA AVAILABILITY

The data that support the findings of this study are available within the article.

REFERENCES

[1]M. Maslov, D. B. King, E. Viezzer, D. L. Keeling, C. Giroud, T. Tala, A. Salmi, M. Marin, J. Citrin, C. Bourdelle, E. R. Solano, and JET Contributors, Nucl. Fusion **58**, 076022 (2018).

[2]C. Angioni, Plasma Phys. Controlled Fusion **63**, 073001 (2021).

05 June 2024 09:58:47

© Author(s) 2024

[3]S. Mazzi, J. Garcia, D. Zarzoso, Y. O. Kazakov, J. Ongena, M. Dreval, M. Nocente, Z. Stancar, G. Szepesi, J. Eriksson, A. Sahlberg, S. Benkadda, and JET Contributors, Nat. Phys. **18**, 776 (2022).
[4]H. Han, S. J. Park, C. Sung, J. Kang, Y. H. Lee, J. Chung, T. S. Hahm, B. Kim, J.-K. Park, J. G. Bak, M. S. Cha, G. J. Choi, M. J. Choi, J. Gwak, S. H. Hahn, J. Jang, K. C. Lee, J. H. Kim, S. K. Kim, W. C. Kim, J. Ko, W. H. Ko, C. Y. Lee, J. H. Lee, J. P. Lee, K. D. Lee, Y. S. Park, J. Seo, S. M. Yang, S. W. Yoon, and Y.-S. Na, Nature **609**, 269 (2022).
[5]K. Ida, M. Yoshinuma, M. Osakabe, K. Nagaoka, M. Yokoyama, H. Funaba, C. Suzuki, T. Ido, A. Shimizu, I. Murakami, N. Tamura, H. Kasahara, Y. Takeiri, K. Ikeda, K. Tsumori, O. Kaneko, S. Morita, M. Goto, K. Tanaka, K. Narihara, T. Minami, I. Yamada, and LHD Experimental Group, Phys. Plasmas **16**, 056111 (2009).
[6]M. Yoshinuma, K. Ida, M. Yokoyama, M. Osakabe, K. Nagaoka, S. Morita, M. Goto, N. Tamura, C. Suzuki, S. Yoshimura, H. Funaba, Y. Takeiri, K. Ikeda, K. Tsumori, O. Kaneko, and LHD Experimental Group, Nucl. Fusion **49**, 062002 (2009).
[7]K. Fujita, S. Satake, M. Nunami, J. M. García-Regaña, J. L. Velasco, and I. Calvo, Nucl. Fusion **61**, 086025 (2021).
[8]F. Nespoli, S. Masuzaki, K. Tanaka, N. Ashikawa, M. Shoji, E. P. Gilson, R. Lunsford, T. Oishi, K. Ida, M. Yoshinuma, Y. Takemura, T. Kinoshita, G. Motojima, N. Kenmochi, G. Kawamura, C. Suzuki, A. Nagy, A. Bortolon, N. A. Pablant, A. Mollen, N. Tamura, D. A. Gates, and T. Morisaki, Nat. Phys. **18**, 350 (2022).
[9]T. Singh, J. H. Nicolau, F. Nespoli, G. Motojima, Z. Lin, A. Sen, S. Sharma, and A. Kuley, Nucl. Fusion **64**, 016007 (2024).
[10]O. Motojima, N. Ohyabu, A. Komori, O. Kaneko, H. Yamada, K. Kawahata, Y. Nakamura, K. Ida, T. Akiyama, N. Ashikawa *et al.*, Nucl. Fusion **43**, 1674 (2003).
[11]M. Salewski, S. K. Nielsen, H. Bindslev, V. Furtula, N. N. Gorelenkov, S. B. Korsholm, F. Leipold, F. Meo, P. K. Michelsen, D. Moseev, and M. Stejner, Nucl. Fusion **51**, 083014 (2011).
[12]M. Salewski, B. Geiger, S. K. Nielsen, H. Bindslev, M. García-Muñoz, W. W. Heidbrink, S. B. Korsholm, F. Leipold, F. Meo, P. K. Michelsen, D. Moseev, M. Stejner, G. Tardini, and ASDEX Upgrade Team, Nucl. Fusion **52**, 103008 (2012).
[13]M. Nishiura, S. Kubo, K. Tanaka, R. Seki, S. Ogasawara, T. Shimozuma, K. Okada, S. Kobayashi, T. Mutoh, K. Kawahata, T. Watari, T. Saito, Y. Tatematsu, S. B. Korsholm, M. Salewski, and LHD Experiment Group, Nucl. Fusion **54**, 023006 (2014).
[14]M. Nishiura, K. Tanaka, S. Kubo, T. Saito, N. Kenmochi, H. Nuga, R. Seki, T. Shimozuma, Y. Yoshimura, H. Igami, H. Takahashi, T. I. Tsujimura, R. Yanai, Y. Tatematsu, and LHD Experiment Group, J. Instrumentation **15**, C01002 (2020).
[15]M. Nishiura, S. Adachi, K. Tanaka, S. Kubo, N. Kenmochi, T. Shimozuma, R. Yanai, T. Saito, H. Nuga, and R. Seki, Rev. Sci. Instrum. **93**, 053501 (2022).
[16]H. Nozato, S. Morita, M. Goto, A. Ejiri, and Y. Takase, Rev. Sci. Instrum. **74**, 2032 (2003).
[17]P. Vincenzi, T. Bolzonella, S. Murakami, M. Osakabe, R. Seki, and M. Yokoyama, Plasma Phys. Controlled Fusion **58**, 125008 (2016).
[18]T. Ido, A. Shimizu, M. Nishiura, K. Nagaoka, M. Yokoyama, K. Ida, M. Yoshinuma, K. Toi, K. Itoh, H. Nakano, S. Nakamura, F. Watanabe, S. Satake, Y. Yoshimura, M. Osakabe, K. Tanaka, T. Tokuzawa, Y. Takeiri, K. Tsumori, K. Ikeda, S. Kubo, T. Shimozuma, H. Igami, H. Takahashi, N. Tamura, and LHD Experiment Group, Plasm Phys. Controlled Fusion **52**, 124025 (2010).
[19]H. Yamaguchi and S. Murakami, Nucl. Fusion **56**, 026003 (2016).
[20]A. Wakasa, S. Murakami, and S. Oikawa, Plasma Fusion Res. **3**, S1030 (2008).
[21]T.-H. Watanabe and H. Sugama, Nucl. Fusion **46**, 24 (2006).

05 June 2024 09:58:47

© Author(s) 2024